

Research Paper

Cite this article: Álvarez-Ortega S, Subbotin SA, Peña-Santiago R (2020). Morphological and molecular characterization of two new species of the genus *Aporcelinus* Andrassy, 2009 (Nematoda, Dorylaimida, Aporcelaimidae) from the USA, with new insights on the phylogeny of the genus. *Journal of Helminthology* **94**, e22, 1–10. <https://doi.org/10.1017/S0022149X18001128>

Received: 8 October 2018

Accepted: 15 November 2018

Key words:

Bayesian inference; description; D2-D3 expansion segments; LSU ribosomal RNA gene; maximum likelihood; molecular; morphology; morphometrics; SEM; taxonomy

Author for correspondence:

S. Álvarez-Ortega, E-mail: sergio.aortega@urjc.es

Morphological and molecular characterization of two new species of the genus *Aporcelinus* Andrassy, 2009 (Nematoda, Dorylaimida, Aporcelaimidae) from the USA, with new insights on the phylogeny of the genus

S. Álvarez-Ortega^{1,2}, S.A. Subbotin² and R. Peña-Santiago³

¹Departamento de Biología y Geología, Física y Química Inorgánica, Universidad Rey Juan Carlos, Campus de Móstoles, 28933-Madrid, España; ²Plant Pest Diagnostics Center, California Department of Food and Agriculture, 3294 Meadowview Road, Sacramento, CA 95832-1448, USA and ³Departamento de Biología Animal, Biología Vegetal y Ecología, Universidad de Jaén, Campus 'Las Lagunillas' s/n, Edificio B3, 23071- Jaén, Spain

Abstract

Two new species of the genus *Aporcelinus* from the USA are described and illustrated. *Aporcelinus floridensis* sp. n. is characterized by its 1.12–1.52 mm long body, lip region offset by marked constriction and 14.5–17.0 µm broad with perioral liplets, odontostyle 16.5–20.0 µm at its ventral side and 1.1–1.2 times the lip region diameter, neck 316–395 µm long, pharyngeal expansion occupying 43–48% of total neck length, uterus simple and 33–56 µm long or 0.8–1.2 times the corresponding body diameter, $V = 48–54$, female tail conical (36–49 µm long, $c = 27–41$, $c' = 1.2–2.0$) with finely rounded terminus and no hyaline portion, and male absent. *Aporcelinus paolae* sp. n. is characterized by its 1.29–1.80 mm long body, lip region offset by marked constriction and 14–16 µm broad, odontostyle 15–17 µm at its ventral side and 1.0–1.1 times the lip region diameter, neck 314–397 µm long, pharyngeal expansion occupying 43–53% of total neck length, uterus tripartite and 128–164 µm long or 2.6–3.6 times the corresponding body diameter, $V = 53–57$, female tail conical (30–39 µm long, $c = 40–51$, $c' = 1.1–1.3$) with finely rounded terminus and variably re-curved dorsad, male tail conical (27–36 µm, $c = 39–59$, $c' = 0.9–1.2$), ventrally straight and dorsally convex, spicules 48–54 µm long, and 7–9 irregularly spaced ventromedian supplements lacking hiatus. The analyses of the D2-D3 expansion segments of 28S rRNA (LSU) gene sequences of the two new species confirmed the monophyly of the genus, based upon currently available data, showing a close relationship between the genera *Aporcelinus* and *Makatinus*, and justified the placement of *Aporcelaimellus*, *Makatinus* and *Aporcelinus* under the subfamily Aporcelaimellinae.

Introduction

Andrassy (2009a) created the genus *Aporcelinus* with nine species, two new and seven transferred. Since its proposal, the genus has received new incorporations (Andrassy, 2009b, 2012; Álvarez-Ortega and Peña-Santiago, 2013; Nguyen *et al.*, 2016a, b; Peña-Santiago and Abolafia, 2016; Varela-Benavides and Peña-Santiago, 2018) and its taxonomic position has been a matter of some controversy (Vinciguerra *et al.*, 2014). To date, the genus *Aporcelinus* contains 26 valid species plus two *species inquirendae*. Available molecular data are limited to only three of its representatives, which is a serious handicap to clarifying the evolutionary relationships with other members of the family Aporcelaimidae Heyns, 1965.

Fortunately, two soil samples, one from Kansas and another from Florida, received in 2011 for nematological inspection by the Nematology Laboratory at the Plant Pest Diagnostics Center, California Department of Food and Agriculture, yielded fresh specimens of two putative new, non-described *Aporcelinus* species. Both species are morphologically and molecularly characterized here.

Materials and methods

Sampling, extraction and morphological identification

Nematodes were extracted from soil samples by sieving and a sucrose centrifugation technique, somewhat modified (specific density = 1.18), according to Barker (1985), relaxed and killed by heat, fixed in 4% formaldehyde, and processed to anhydrous glycerin following the technique

of Siddiqi (1964). The specimens were mounted on permanent glass slides for observation under a light microscope.

Specimens were examined and measured using an Olympus BH-2 light microscope equipped with differential interference contrast (DIC). Morphometrics included de Man's indices and standard measurements. The location of the pharyngeal gland nuclei was expressed according to Loof and Coomans (1970) and the spicule terminology was according to Peña-Santiago *et al.* (2014). Some of the best-preserved specimens were photographed with a Nikon Eclipse 80i microscope equipped with DIC and a Nikon DS digital camera. Digital images were edited using Adobe® Photoshop® CS. Drawings were made using a camera lucida attached to the microscope. After their examination and identification, one specimen of the new species *Aporcelinus paolae* sp. n. preserved in glycerin was selected for examination by scanning electron microscopy (SEM) following the protocol of Álvarez-Ortega and Peña-Santiago (2016). The nematode was hydrated in distilled water, dehydrated in a graded ethanol and acetone series, critical point-dried, coated with gold, and observed under a Zeiss Merlin microscope.

DNA extraction, polymerase chain reaction (PCR) and sequencing

DNA was extracted from a single individual using the proteinase K protocol. Nematode material was transferred to an Eppendorf tube containing 30 µl double distilled water, 3 µl polymerase chain reaction (PCR) buffer (Qiagen, Hilden, Germany) and 2 µl proteinase K (600 µg ml⁻¹) (Qiagen). The tubes were incubated at 65°C (1 h) and then at 95°C (15 minutes). PCR and sequence protocols were as described by Álvarez-Ortega *et al.* (2013a). The primers used for amplification of the D2-D3 expansion segments of 28S rRNA gene were the D2A (5'-ACAAGTACCGTGAGGGAAAGTTG-3') and the D3B (5'-TCGGAAGGAACCAGCTACTA-3') primers (Subbotin *et al.*, 2006).

PCR products were purified using the QIAquick PCR purification Kit (Qiagen) and used for direct sequencing. The sequencing reactions were performed at Davis Sequencing (Davis, CA, USA). The sequences obtained were submitted to the GenBank database under accession numbers MK007552 and MK007553.

Phylogenetic analyses

The newly obtained sequences were aligned with the other 58 D2-D3 expansion segments of 28S rRNA gene sequences available in GenBank using ClustalX 1.83 (Thompson *et al.*, 1997). Outgroup taxa were chosen according to the results of previous published data (Holterman *et al.*, 2008; Álvarez-Ortega *et al.*, 2013b). Sequence alignments were manually edited using GenDoc 2.6.002 (Nicholas *et al.*, 1997). Bayesian inference (BI) and maximum-likelihood (ML) analyses of the sequence dataset were performed at the CIPRES Science Gateway (Miller *et al.*, 2010), using MrBayes 3.2.6 (Ronquist *et al.*, 2012) and RAxML 8.2.10 (Stamatakis, 2014), respectively. The best fit model of DNA evolution was obtained using jModelTest 2.1.10 (Darriba *et al.*, 2012) with the Akaike information criterion (AIC). The Akaike-supported model, the base frequency, the proportion of invariable sites, and the gamma distribution shape parameters and substitution rates in the AIC were then used in phylogenetic analyses. BI analysis under the general time reversible model with a proportion of invariable sites and a gamma-shaped distribution (GTR + I + G) was initiated with a random starting tree and run

with the four Metropolis-coupled Markov chain Monte Carlo (MCMC) for 2×10^6 generations. ML analysis was implemented under the same nucleotide substitution model as in the BI, with 1000 bootstrap replications. The topologies were used to generate a 50% majority rule consensus tree. Posterior probabilities (PP) and bootstrap support (BS) over 70% are given on appropriate clades. The trees were visualized using the program FigTree v1.4.3, and drawn with Adobe Acrobat XI Pro 11.0.1.

Results

Aporcelinus floridensis sp. n. (figs 1 and 2)

Material examined

Twelve females from one location, in variable (in general acceptable) states of preservation.

Morphometrics

See table 1.

Description

Female. Moderately slender ($a = 25\text{--}29$) nematodes of medium size, 1.12–1.52 mm long. Habitus curved ventrad upon fixation, in general, C-shaped. Cuticle two-layered, 2.0–2.5 µm thick at anterior region, 2.5–3.5 µm in mid-body and 3.0–4.5 µm on tail; outer layer thin and bearing fine but conspicuous transverse striation throughout the body; inner layer thicker and more refractive than the outer layer. Lateral chord 6–10 µm broad or 13–21% of mid-body diameter. Body pores often obscure under light microscope. Lip region offset by a distinct constriction, 2.9–3.4 times as wide as high and 32–37% of body diameter at neck base; labial and cephalic papillae slightly protruding; oral field visibly elevated, suggesting the existence of perioral liplets. Amphid fovea funnel-shaped, its opening 8–10 µm broad or 52–63% of lip region diameter. Cheilostome nearly as long as wide, with no specialization. Odontostyle strong, slightly longer (1.1–1.2 times) than lip region diameter, 5.8–7.8 times longer than wide and 1.15–1.56% of total body length; aperture 9.0–10.5 µm or 51–56% of its total length. Guiding ring simple but distinct and somewhat plicate, located at 8.0–10.5 µm or 0.5–0.6 times the lip region diameter from the anterior end. Odontophore rod-like, 1.6–2.2 times the odontostyle long. Pharynx consisting of a slender but muscular anterior section enlarging very gradually in the posterior, the expansion 4.9–6.7 times as long as wide, 2.8–4.0 times the corresponding body diameter and occupies 43–48% of total neck length; gland nuclei in general obscure in the specimens examined: DN = 66–69, S₁N₁ = 71–75, S₁N₂ = 78–82, S₂N = 88–93. Nerve ring at 119–142 µm or 36–40% of total neck length from the anterior end. Pharyngo-intestinal junction surrounded by an asymmetrical ring-like structure, with a distinctly developed dorsal lobe; cardia conical, 17–23 × 10–15 µm; a dorsal cell mass is present at a variable distance behind the pharyngeal base. Genital system didelphic–amphidelphic, with both branches equally and well developed, 104–199 µm long or 9–14% of total body length; ovaries 60–190 µm long, often not reaching the oviduct–uterus junction; oviduct 54–78 µm long or 1.2–1.5 times the body diameter, and consisting of a slender portion and a small *pars dilatata* with visible lumen; a sphincter separates oviduct and uterus; uterus a short and simple tube-like structure 33–56 µm long or 0.8–1.2 times the corresponding body diameter, without sperm cells observed inside; vagina extending inwards 19–24 µm or 38–49% of body diameter, with *pars proximalis* 10–15 ×

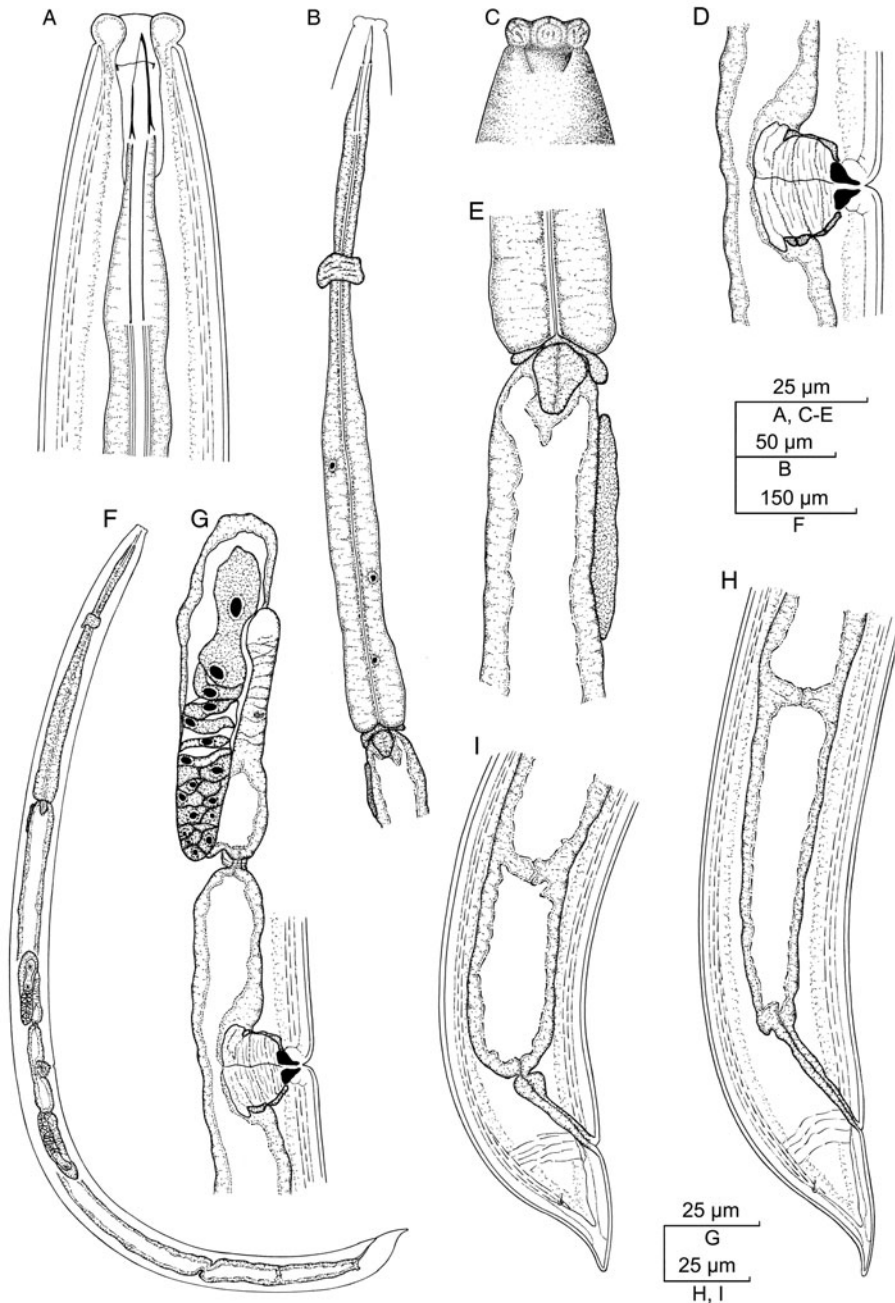


Fig. 1. *Aporcelinus floridensis* sp. n. (female, line drawing). (A) Anterior region in lateral median view; (B) neck region; (C) lip region in lateral surface view; (D) vagina; (E) pharyngo-intestinal junction; (F) entire body; (G) anterior genital branch; (H, I) posterior body region.

13–21 µm and convergent walls surrounded by weak musculature, *pars refringens* consisting of two drop-shaped to trapezoidal pieces 4.5–7.0 × 3.0–4.5 µm and a combined width of 6.5–10.0 µm, and *pars distalis* 4.5–6.5 µm long and visibly refractive; and vulva a transverse slit. Prerectum 1.7–3.2 and rectum 1.0–1.4 times the anal body diameter long. Tail conical with finely rounded tip, ventrally straight or slightly convex, dorsally first convex and then bearing a more or less conspicuous concavity and re-curved dorsad; inner cuticle layer reaching the tail tip, so that a hyaline portion is not perceptible; caudal pores two pairs at the middle of tail, one subdorsal, another sublateral.

Male. Unknown.

Molecular characterization

One sequence of the D2-D3 of 28S rRNA gene 747 bp long was obtained. The evolutionary relationships of the new species with several representatives of the order Dorylaimida are presented in fig. 3.

Diagnosis

This new species is characterized by its 1.12–1.52 mm long body, lip region offset by marked constriction and 14.5–17.0 µm broad with perioral liplets, odontostyle 16.5–20.0 µm at its ventral side and 1.1–1.2 times the lip region diameter, neck 316–395 µm long, pharyngeal expansion 142–191 µm long or 43–48% of

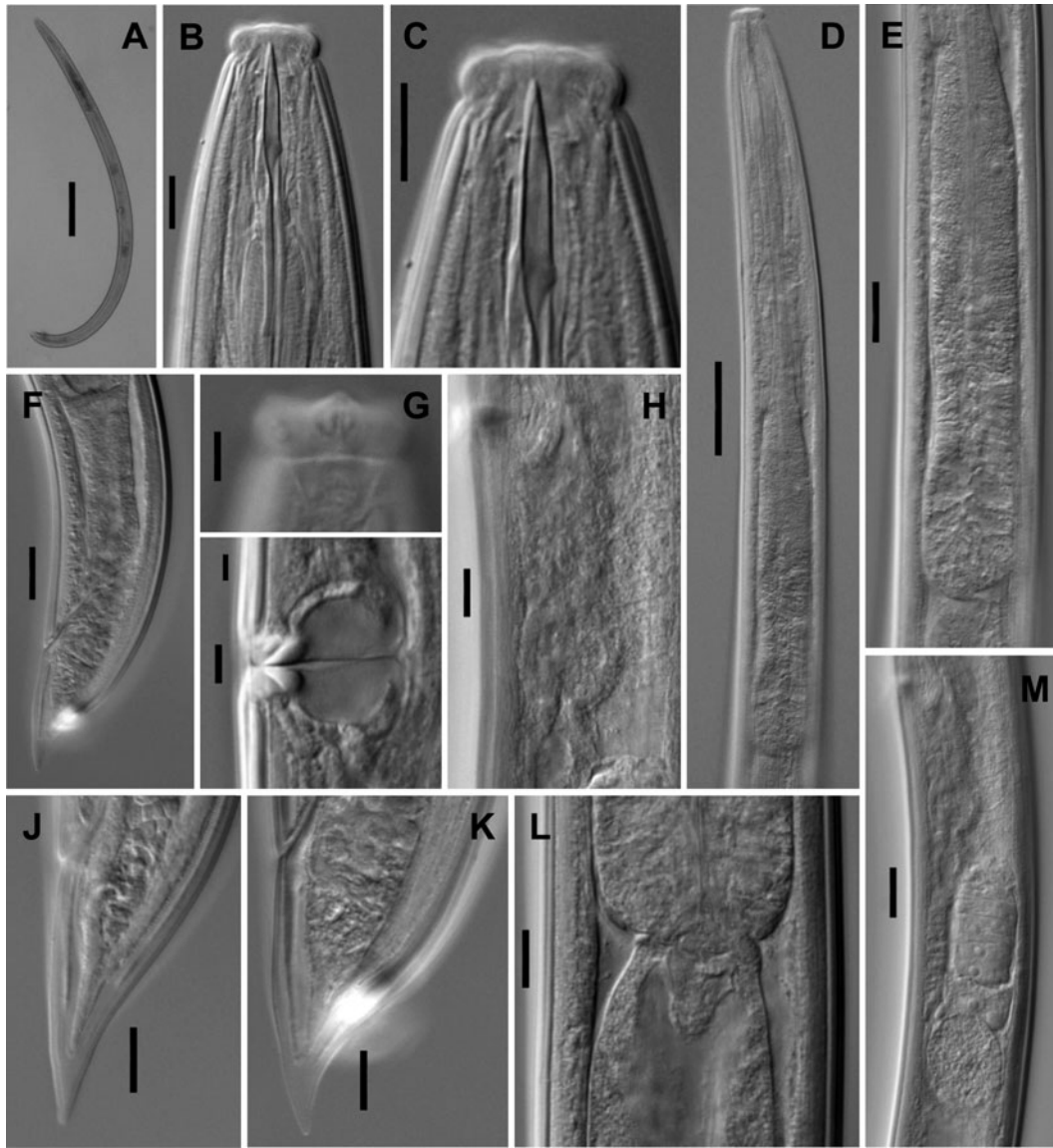


Fig. 2. *Aporcelinus floridensis* sp. n. (female, light micrographs). (A) entire body; (B, C) anterior region in lateral median view; (D) neck region; (E) pharyngeal expansion; (F) caudal region and prerectum; (G) lip region in surface lateral view; (H) uterus; (I) vagina; (J, K) caudal region; (L) pharyngo-intestinal junction; (M) posterior genital branch. (Scale bars: A = 200 μ m; B, C, H, J–L = 10 μ m; D = 50 μ m; E, F, M = 20 μ m; G, I = 5 μ m)

total neck length, a dorsal cell mass present at variable distance behind the level of pharyngo-intestinal junction, uterus simple and 33–56 μ m long or 0.8–1.2 times the corresponding body diameter, $V = 48$ –54, female tail conical (36–49 μ m, $c' = 27$ –41, $c'' = 1.2$ –2.0) with finely rounded terminus and no hyaline portion, and male absent.

Relationships

In having medium general size (body length almost always > 1.0 mm), comparatively small odontostyle (up to 22 μ m long) and female tail bearing a distinct dorsal concavity and ending in a finely rounded terminus, the new species resembles *A. irritans* (Cobb *in* Thorne & Swanger, 1936) Andr ssy, 2009, *A. jiaonanensis* (Zhao & Zhao, 2010)  lvarez-Ortega & Pe a-Santiago, 2013 (see recent description by Nguyen *et al.*, 2017) and *A. neogranuliferus* Pe a-Santiago & Abolafia, 2016, a group of species with intricate taxonomy. It differs from *A. irritans* in its less angular

and broader lip region (exceptionally under 15.5 vs 14–15 μ m), shorter odontostyle (up to 20 vs 20–21 μ m, 1.1–1.2 vs 1.4 times the lip region diameter), shorter female prerectum (up to 1.4 vs twice the anal body diameter long), and male absent (vs present); from *A. jiaonanensis* in its narrower lip region (up to 17 vs 17–20 μ m wide), shorter odontostyle (up to 20 vs 20–23 μ m long), comparatively shorter pharyngeal expansion (43–48 vs 47–55% of total neck length), shorter uterus (33–56 vs 56–97 μ m long), comparatively longer female tail ($c' = 1.2$ –2.0 vs $c' = 0.7$ –1.3) without (vs with) hyaline terminal portion, male unknown (vs known), and in remarkable differences in partial sequences of D2–D3 of LSU rRNA gene; and from *A. neogranuliferus*, a very similar species, in its narrower lip region (14.5–17.0 vs 17.5–18.0 μ m broad), slightly longer odontostyle (1.1–1.2 times vs equal to the lip region diameter) with larger aperture (51–56 vs 46–51% of total length), and longer female tail (36–49 vs 28–35 μ m, $c' = 1.2$ –2.0 vs 0.8–1.0).

Table 1. Morphometrics of *Aporcelinus floridensis* sp. n. and *A. paolae* sp. n. Measurements in μm (except L, in mm), and in the form of mean \pm standard deviation (range).

Character	<i>A. floridensis</i> sp. n.				<i>A. paolae</i> sp. n.			
	n	Florida, USA		Kansas, USA		♂	8♂♂	
		Holotype	Paratypes	Holotype	Paratypes			
		♀	11♀♀	♀	3♀♀			
L	1.52	1.32 \pm 0.11 (1.12–1.52)	1.67	1.61 \pm 0.17 (1.46–1.80)	1.46	1.46 \pm 0.11 (1.29–1.65)		
a	28	27.0 \pm 1.2 (25–29)	36	32.1 \pm 3.4 (29–35)	35	32.8 \pm 2.8 (28–36)		
b	3.8	3.7 \pm 0.2 (3.4–4.1)	4.4	4.3 \pm 0.3 (3.9–4.5)	4.1	4.3 \pm 0.2 (4.1–4.8)		
c	34	32.2 \pm 3.9 (27–41)	51	44.9 \pm 4.0 (40–48)	50	48.8 \pm 5.7 (39–59)		
c'	1.4	1.5 \pm 0.2 (1.2–2.0)	1.2	1.2 \pm 0.1 (1.1–1.3)	1.1	1.1 \pm 0.1 (0.9–1.2)		
V	52	52.0 \pm 0.0 (48–54)	55	54.4 \pm 2.1 (53–57)	–	–		
Lip region diameter	16.5	15.9 \pm 0.7 (14.5–17.0)	16	15.0 \pm 0.0 (15–15)	14	14.7 \pm 0.3 (14–15)		
Odontostyle length at ventral side	17.5	18.2 \pm 1.1 (16.5–20.0)	16	16.0 \pm 0.7 (16–17)	16	15.6 \pm 0.4 (15–16)		
Odontophore length	39	35.0 \pm 2.0 (32–39)	29	31.3 \pm 1.3 (30–32)	29	30.1 \pm 1.0 (29–32)		
Neck length	395	354 \pm 25 (316–395)	378	375 \pm 20 (356–397)	360	339 \pm 17 (314–360)		
Pharyngeal expansion length	182	164 \pm 16 (142–191)	166	180 \pm 8 (174–190)	172	159 \pm 13 (145–185)		
Body diameter at neck base	52	46.1 \pm 3.6 (39–52)	42	47.3 \pm 1.3 (46–49)	40	42.6 \pm 2.5 (40–46)		
Body diameter at mid body	55	49.0 \pm 4.1 (41–55)	46	50.2 \pm 0.7 (49–51)	42	44.5 \pm 2.6 (42–47)		
Body diameter at anus/cloaca	32	27.8 \pm 3.1 (22–32)	28	29.7 \pm 2.2 (27–31)	26	27.9 \pm 1.7 (26–30)		
Prerectum length	62	67.9 \pm 13.9 (51–94)	95	70.4 \pm 10.3 (60–81)	?	140 \pm 21 (111–159)		
Rectum/cloaca length	31	34.9 \pm 3.4 (30–42)	44	37.2 \pm 2.6 (34–40)	48	45.5 \pm 1.6 (43–48)		
Tail length	33	41.4 \pm 4.3 (36–49)	33	36.0 \pm 5.0 (30–39)	29	30.1 \pm 2.4 (27–36)		
Spicule length	–	–	–	–	48	50.7 \pm 2.4 (48–54)		
Ventromedian supplements	–	–	–	–	8	(7–9)		

Type locality and habitat

Fort Pierce, Florida, USA, where the new species was collected in association with *Ficus benjamina*.

Type material

Female holotype, nine female paratypes deposited in the nematode collection of the University of Jaén, Spain. Two female paratypes deposited with the USDA Nematode Collection, Beltsville, MD, USA.

Etymology

The specific epithet refers to the geographical origin of the species.

Aporcelinus paolae sp. n. (figs 4–6)

Material examined

Four females and nine males from one location, in good state of preservation.

Morphometrics

See table 1.

Description

Adult. Moderately slender to slender ($a = 28$ – 36) nematodes of medium size, 1.29–1.80 mm long. Habitus visibly curved ventrad

upon fixation, in general C-shaped. Cuticle two-layered, 2.0–2.5 μm thick at anterior region, 2.5–3.0 μm in mid-body and 2.5–4.0 μm on tail; outer layer thin and bearing fine but conspicuous transverse striation throughout the body; inner layer thicker and more refractive than the outer layer. Lateral chord 6–10 μm broad or 12–20% of mid-body diameter. Body pores often obscure, but two cervical pores are visible at both dorsal and ventral sides at level of odontostyle plus odontophore. Lip region moderately angular, offset by a distinct constriction, 3.2–3.5 times as wide as high and 31–37% of body diameter at neck base. Under SEM: lips mostly amalgamated, separated by marked interlabial depressions, each lip bearing two or three concentric incisures at its inner (oral field) part and five to six at its outer part; labial papillae button-like with a pore in the centre, with both inner and outer papillae equally sized and surrounded by a coarse annulus; cephalic papillae opening in a short transverse slit, which is not surrounded by a coarse annulus similar to that found in labial papillae; oral field poorly differentiated by a very weak elliptical (or somewhat hexagonal) incisure, bearing coarse radial striation ending at the base of the lips; oral opening a relatively short dorsoventral slit. Amphid fovea cup-shaped, its opening 7.0–8.5 μm broad or 48–56% of lip region diameter. Cheilostom nearly as long as wide, with no specialization. Odontostyle strong, nearly equal (1.0–1.1 times) to lip region diameter, 6.1–6.9 times longer than wide and 0.96–1.24% of

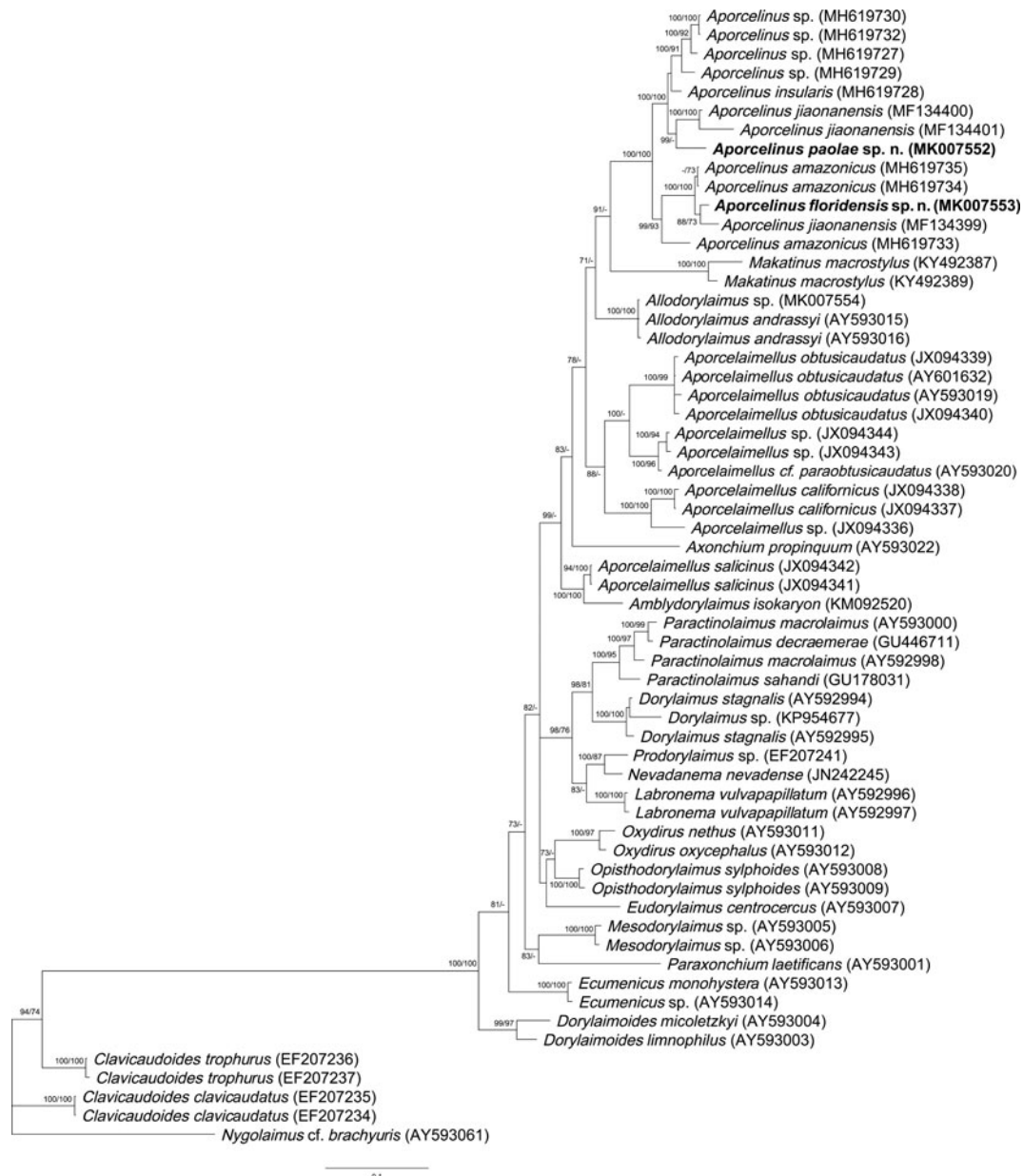


Fig. 3. Bayesian 50% majority rule consensus tree as inferred from the D2-D3 expansion segments of 28S rRNA gene sequence alignments under the GTR + I + G model. Branch support of over 70% is given for appropriate clades and is indicated as posterior probability value in Bayesian inference analysis/bootstrap value from maximum-likelihood analysis. Newly obtained sequences are indicated by bold letters.

total body length; aperture 7.5–9.0 μm or 47–54% of its total length. Guiding ring simple but distinct and somewhat plicate, located at 6.5–8.0 μm or 0.4–0.6 times the lip region diameter from the anterior end. Odontophore rod-like, 1.8–2.0 times the odontostyle long. Pharynx consisting of a slender but muscular anterior section enlarging very gradually in the posterior expansion that is 6.0–8.0 times as long as wide, 3.2–4.5 times the corresponding body diameter and occupies 43–53% of total neck length; most of the gland nuclei are obscure in the specimens examined: DN = 65–68, S_2N = 89. Nerve ring at 114–147 μm or 33–39% of total neck length from the anterior end. Pharyngo-intestinal junction surrounded by an asymmetrical ring-like structure, with a distinctly developed dorsal lobe; cardia conical, 12–14 \times 9–11 μm ; a dorsal cell mass is present at variable distance behind the pharyngeal base.

Female. Genital system didelphic–amphidelphic, with both branches equally and very well developed, 231–277 μm long or 15–17% of total body length; ovaries 96–118 μm long, often not reaching the oviduct–uterus junction; oviduct 88–117 μm long or 1.7–2.3 times the body diameter, and consisting of a slender portion and a large *pars dilatata* with wide lumen and abundant sperm cells inside; a sphincter separates oviduct and uterus; uterus 128–164 μm long or 2.6–3.6 times the corresponding body diameter, tripartite, that is consisting of a short and wider proximal region, a narrower intermediate section with very narrow lumen, and a nearly spherical large distal part; vagina extending inwards 25–28 μm or 51–55% of body diameter, with *pars proximalis* 17–19 \times 15–18 μm and somewhat sigmoid walls surrounded by weak musculature, *pars refringens* consisting of two drop-shaped to trapezoidal pieces 5–7 \times 2–3.5 μm and a

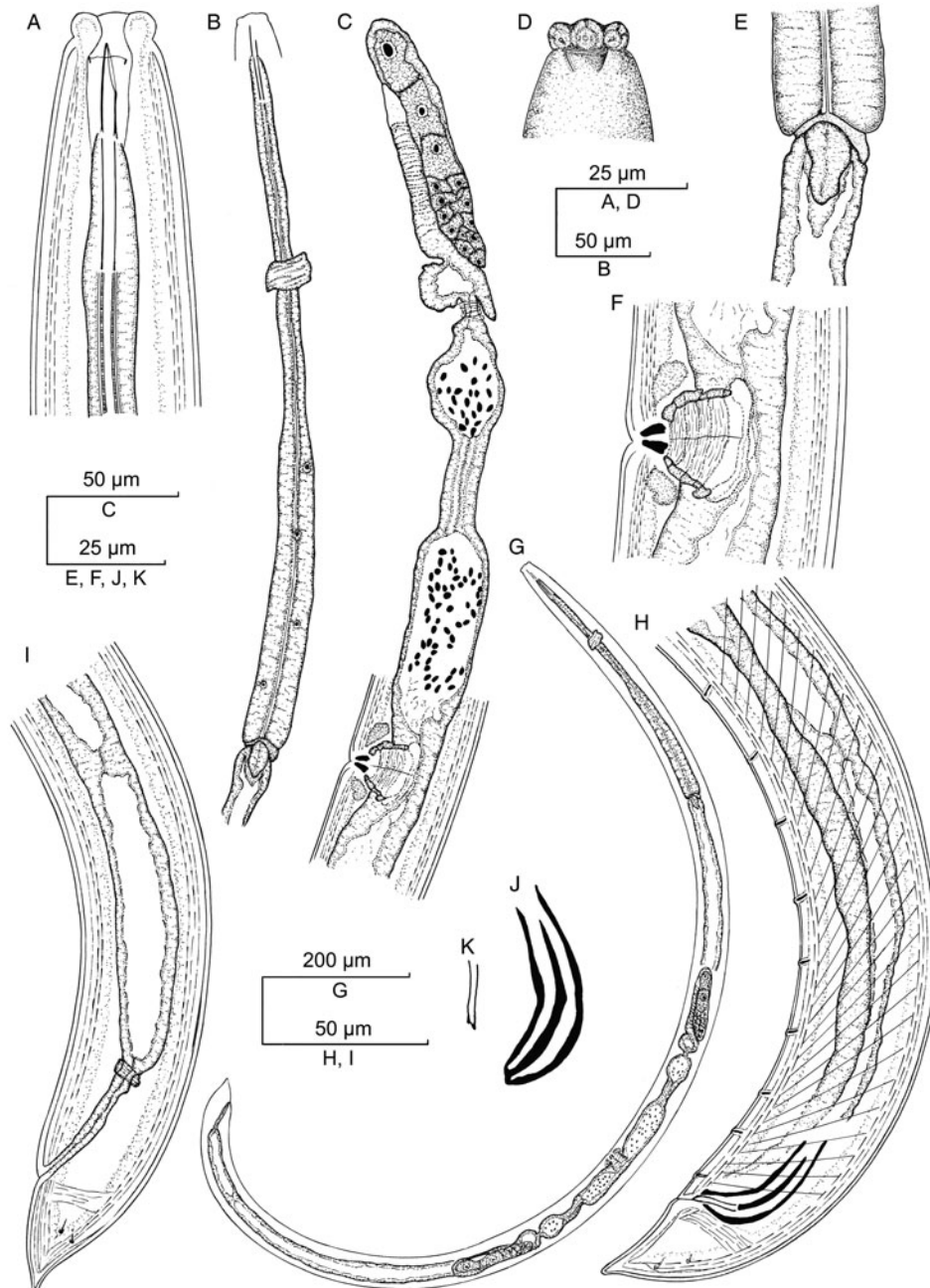


Fig. 4. *Aporcelinus paolae* sp. n. (line drawing). (A) Anterior region in lateral median view; (B) neck region; (C) female, anterior genital branch; (D) lip region in lateral surface view; (E) pharyngo-intestinal junction; (F) vagina; (G) female, entire; (H) male, posterior body region; (I) female, posterior body region; (J) spicule; (K) lateral guiding piece.

combined width of 6–7 μm , and *pars distalis* 4–5 μm long and visibly refractive; vulva a transverse slit. Prerectum 2.0–2.4 and rectum 1.1–1.6 times the anal body diameter long. Tail conical with finely rounded tip, ventrally convex, dorsally first convex and then bearing a more or less conspicuous concavity and re-curved dorsad; inner cuticle layer not reaching the tail tip, so that a hyaline portion up to 8 μm thick is perceptible; caudal pores two pairs at the middle of tail, one subdorsal, another sublateral.

Male. Genital system diorchic, with opposite testes. In addition to the ad-cloacal pair, situated at 7.5–11.0 μm from the cloacal aperture, there is a series of 7–9 irregularly spaced, 8–21 μm apart, ventromedian supplements, one (often) or two (rarely) of them located within the range of spicules, at 16–19 μm from

the ad-cloacal pair. Spicules dorylaimoid, 4.8–5.5 times as long as wide, and 1.7–2.1 times longer than anal body diameter. Curvature 130–139°. Dorsal side regularly convex, ventral side lacking distinct hump and hollow. Head 1.3–1.6 times longer than wide, occupying 17–21% of total length, its dorsal side hardly longer than the ventral side, both sides nearly straight. Median piece 14–17 times longer than wide, occupying 25–29% of the spicule maximum width, reaching the terminal tip. Posterior end 3.0–4.0 μm wide. Lateral guiding pieces 10–11 μm long, 4.9–6.0 times longer than wide. Prerectum 3.7–6.0 and cloaca 1.4–1.9 times the corresponding body width long. Tail conical with finely rounded tip, ventrally straight or slightly curved ventrad, dorsally regularly convex; inner cuticle layer not reaching



Fig. 5. *Aporcelinus paolae* sp. n. (light micrographs). (A) female, entire; (B) male, entire; (C–E) anterior region in lateral median view; (F) lip region in lateral surface view; (G) female, anterior genital branch; (H) pharyngo-intestinal junction, arrow head pointing at dorsal cell mass; (I, K) spicule; (J) lateral guiding piece; (L) pharyngo-intestinal junction; (M) female, caudal region; (N) male, posterior body region; (O) vagina; (P, Q) male, caudal region. (Scale bars: A, B = 200 μ m; C, D, I, K, L, M, O–Q = 10 μ m; E, F = 5 μ m; G = 50 μ m; H, N = 20 μ m; J = 2 μ m)

the tail tip, so that a hyaline terminal portion, up to 10 μ m thick is perceptible; inner core of tail often bearing a dorsal, terminal indentation; caudal pores two pairs at the middle of tail, one sub-dorsal, another sublateral.

Molecular characterization

One sequence of the D2-D3 28S rRNA gene 754 bp long was obtained. The evolutionary relationships of the new species with several representatives of the order Dorylaimida are presented in fig. 3.

Diagnosis

This new species is characterized by its 1.29–1.80 mm long body, lip region offset by marked constriction and 14–16 μ m broad, odontostyle 15–17 μ m at its ventral side or 1.0–1.1 times the lip

region diameter, neck 314–397 μ m long, pharyngeal expansion 145–190 μ m long or 43–53% of total neck length, a dorsal cell mass present at variable distance behind the level of pharyngo-intestinal junction, uterus tripartite and 128–164 μ m long or 2.6–3.6 times the corresponding body diameter, $V = 53$ –57, female tail conical (30–39 μ m, $c = 40$ –51, $c' = 1.1$ –1.3) with finely rounded terminus and variably re-curved dorsad, male tail conical (27–36 μ m, $c = 39$ –59, $c' = 0.9$ –1.2), ventrally straight and dorsally convex, spicules 48–54 μ m long, and 7–9 irregularly spaced ventromedian supplements lacking hiatus.

Relationships

In having medium general size (body length > 1.0 mm), comparatively small odontostyle (< 22 μ m long) and female tail bearing a

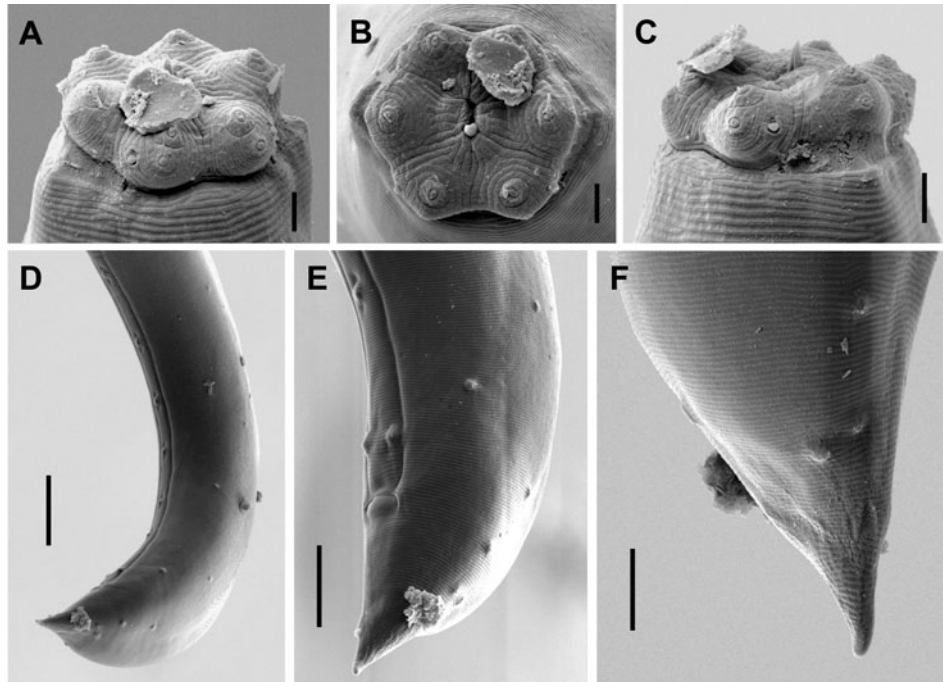


Fig. 6. *Aporcelinus paolae* sp. n. (male, SEM). (A) Lip region in dorsal view; (B) lip region in frontal view; (C) lip region in lateral view; (D) posterior body region; (E) caudal region in subventral view; (F) caudal region in dorsal view. (Scale bars: A–C = 2 μ m; D = 20 μ m; E = 10 μ m; F = 5 μ m)

distinct dorsal concavity and ending in a finely rounded terminus, the new species resembles *A. irritans*, *A. jiaonanensis* and *A. neogranuliferus*. It can be distinguished from *A. irritans*, a poorly known species, by its shorter odontostyle (15–17 vs 20–21 μ m), more posterior vulva ($V = 53$ –57 vs 50), and shorter tail (27–36 vs 39–42 μ m, $c' = 0.9$ –1.2 vs $c' = 1.3$ –1.4); from *A. jiaonanensis* in its narrower lip region (14–16 vs 17–20 μ m), shorter odontostyle (15–17 vs 20–23 μ m), and longer uterus (128–164 vs 56–97 μ m, 2.6–3.6 vs 1.0–1.5 times the corresponding body diameter); and from *A. neogranuliferus* in its narrower lip region (14–16 vs 17–18 μ m), longer (128–164 vs 41–48 μ m, 2.6–3.6 vs 0.6 times the corresponding body diameter) and complex (tripartite vs unipartite) uterus, more posterior vulva ($V = 53$ –57 vs 49–53), presence of a distinct hyaline portion at tail end (inner cuticle layer not reaching vs reaching the tip), and males as frequent as females (vs male absent).

Type locality

Washington Marlatt, Kansas, USA, where the new species was collected in a prairie.

Type material

Female holotype, male allotype, two female and seven male paratypes deposited in the nematode collection of the University of Jaén, Spain. One female and one male paratype deposited with the USDA Nematode Collection, Beltsville, MD, USA.

Etymology

The new species is named after the first author's daughter, Paola.

Discussion

The two new taxa described herein together with *A. irritans*, *A. jiaonanensis* and *A. neogranuliferus* form a group of very similar species, with intricate taxonomy. Their separation may

occasionally be problematic because, in general, it is based on small morphological differences. *Aporcelinus paolae* sp. n. and *A. jiaonanensis* are distinguishable from *A. neogranuliferus* and *A. floridensis* sp. n. by the morphology of their female genital tract (long and tripartite vs short and simple uterus, respectively), a significant difference indeed. Unfortunately, no information is available about the genital tract of *A. irritans*. *Aporcelinus floridensis* sp. n. and *A. neogranuliferus* differ from *A. jiaonanensis* and *A. paolae* sp. n. in lacking (vs bearing) a perceptible hyaline terminal portion at tail, a subtle but appreciable and relevant difference. Unfortunately, again, there are no data on this feature in *A. irritans*. Other differences observed among these species (see relationships above) are morphometrical and small but significant enough to support a provisional separate status for them.

Molecular data of *Aporcelinus* species are still insufficient and are currently limited to only seven sequences belonging to three species (*A. amazonicus* (Andrássy, 2004) Andrásy, 2009 MH619733–35, *A. insularis* (Andrássy, 2004) Álvarez-Ortega & Peña-Santiago, 2013 MH619728 and *A. jiaonanensis* MF134399–401). Additionally, there are four sequences that are currently identified only to genus level (MH619727, MH619729–30 and MH619732). However, these molecular data should be considered with caution, because the available sequences for *A. amazonicus* and *A. jiaonanensis* show remarkable differences between them, and may represent more than one different species (fig. 3).

The inferred phylogenetic tree based on the D2–D3 of 28S rRNA gene sequences is presented in fig. 3. It shows that the new species are clustered together with other *Aporcelinus* sequences in a well-supported clade (posterior probabilities for BI: 100% and bootstrap support for ML: 96%). Besides, the results obtained suggest a close relationship between *Aporcelinus* and the genus *Makatinus* Heyns, 1965, another member of the family Aporcelaimidae. Finally, the genera *Aporcelinus* and *Makatinus* are clustered within a well-supported clade (PP: 91%), which includes other two Aporcelaimidae genera, *Aporcelaimellus* and

Amblydorylaimus Andrásy, 1998, as well as representatives of the genus *Allodorylaimus* Andrásy, 1986, a taxon morphologically quite similar to *Aporcelinus*, and *Axonchium* Cobb, 1920, a genus belonging to the family Belondiridae Thorne, 1939. Therefore, these results confirm a close relationship between *Aporcelinus* and other Aporcelaimidae members, and justify the classification of the genus *Aporcelinus* under this family.

On the other hand, Andrásy (2009a) created the subfamily Aporcelaimellinae to accommodate the genera *Aporcelaimellus*, *Makatinus* and *Aporcelinus*, and justified this action because these three aporcelaimid genera differ from the other representatives of the family Aporcelaimidae in the structure of the cuticle. The molecular results herein support and justify Andrásy's action. Nevertheless, further morphological and molecular studies, using additional DNA markers, are necessary to test and clarify the evolutionary relationship between *Aporcelinus* and *Allodorylaimus*, especially because the latest genus belongs to another dorylaimid family, Qudsianematidae Jairajpuri, 1965.

Author ORCIDs.  S. Álvarez-Ortega 0000-0003-2077-5041.

Acknowledgements. The authors are grateful to Dr Cheryl Blomquist (Sacramento, CA, USA) who collected the soil samples from Kansas. SEM pictures were obtained with the assistance of technical staff and equipment of Centro de Instrumentación Científico-Técnica (CICT) at the University of Jaén (Spain).

Conflict of interest. None.

References

- Álvarez-Ortega S and Peña-Santiago R (2013) Taxonomy of the genus *Aporcelaimellus* Heyns, 1965 (Nematoda, Dorylaimida, Aporcelaimidae). *Zootaxa* **3669**, 243–260. <http://dx.doi.org/10.11646/zootaxa.3669.3.3>
- Álvarez-Ortega S and Peña-Santiago R (2016) *Aporcella charidiemsiensis* sp. n. (Dorylaimida: Aporcelaimidae) from the southern Iberian Peninsula, with comments on the phylogeny of the genus. *Nematology* **18**, 811–821. <http://dx.doi.org/10.1163/15685411-00002995>
- Álvarez-Ortega S, Subbotin SA and Peña-Santiago R (2013a) Morphological and molecular characterisation of *Aporcelaimellus simplex* (Thorne & Swanger, 1936) Loof & Coomans, 1970 and a new concept for the genus *Aporcella* Andrásy, 2002 (Dorylaimida, Aporcelaimidae). *Nematology* **15**, 165–178. <http://dx.doi.org/10.1163/156854112X651320>
- Álvarez-Ortega S, Subbotin SA and Peña-Santiago R (2013b) Morphological and molecular characterisation of Californian species of the genus *Aporcelaimellus* Heyns, 1965 (Dorylaimida: Aporcelaimidae). *Nematology* **15**, 431–439. <http://dx.doi.org/10.1163/15685411-00002691>
- Andrásy I (1986) The genus *Eudorylaimus* Andrásy, 1959 and the present status of its species (Nematoda: Qudsianematidae). *Opuscula Zoologica Budapestinensis* **22**, 1–42.
- Andrásy I (1998) Nematodes in the sixth continent. *Journal of Nematode Morphology and Systematics* **1**, 107–186.
- Andrásy I (2004) Two new species of *Aporcelaimellus* Heyns, 1965 (Nematoda: Dorylaimida) from the tropics. *Acta Zoologica Academiae Scientiarum Hungaricae* **50**, 97–107.
- Andrásy I (2009a) *Aporcelinus*, a new genus of aporcelaimoid nematodes (Dorylaimida), and its species. *International Journal of Nematology* **19**, 121–136.
- Andrásy I (2009b) Another species of the genus *Aporcelinus* Andrásy, 2009 (Nematoda: Dorylaimida). *Opuscula Zoologica Budapestinensis* **40**, 99–102.
- Andrásy I (2012) Two new species of the family Aporcelaimidae (Nematoda: Dorylaimida). *Genus* **23**, 189–199.
- Barker KR (1985) Nematode extraction and bioassays. In Barker KR, Carter CC and Sasser JN (eds), *An Advanced Treatise on Meloidogyne, Volume II. Methodology*. Raleigh, NC: North Carolina State University, pp. 19–35.
- Cobb NA (1920) One hundred new nemas. (Type species of 100 new genera). *Contributions to a Science of Nematology* **9**, 217–243.
- Darriba D et al. (2012) jModelTest 2: more models, new heuristics and parallel computing. *Nature Methods* **9**, 772.
- Heyns J (1965) On the morphology and taxonomy of the Aporcelaimidae, a new family of dorylaimoid nematodes. *Entomology Memoirs, Department of Agricultural Technical Services, Republic of South Africa* **10**, 1–51.
- Holterman M et al. (2008) A ribosomal DNA-based framework for the detection and quantification of stress-sensitive nematode families in terrestrial habitats. *Molecular Ecology Resources* **8**, 23–34. <http://dx.doi.org/10.1111/j.1471-8286.2007.01963.x>
- Jairajpuri MS (1965) *Qudsianema amabilis* n. gen., n. sp. (Nematoda: Dorylaimoidea) from India. *Proceedings of the Helminthological Society of Washington* **31**, 59–64.
- Loof PAA and Coomans A (1970) On the development and location of the oesophageal gland nuclei in Dorylaimina. *Proceedings of the IX International Nematology Symposium (Warsaw, Poland, 1967)*, pp. 79–161.
- Miller M, Pfeiffer W and Schwartz T (2010) Creating the CIPRES Science Gateway for inference of large phylogenetic trees. *Proceedings of the Gateway Computing Environments Workshop (GCE), 2010 (USA)*, pp. 1–8.
- Nguyen TAD et al. (2016a) Two new species of the genus *Aporcelinus* Andrásy, 2009 (Nematoda, Dorylaimida, Aporcelaimidae) from Vietnam. *Zootaxa* **4103**, 550–560. <http://dx.doi.org/10.11646/zootaxa.4103.6.5>
- Nguyen TAD et al. (2016b) A third new species of *Aporcelinus* Andrásy, 2009 (Dorylaimida, Aporcelaimidae) from Vietnam, with the first SEM study of a representative of the genus. *Journal of Nematology* **48**, 104–108. <http://journals.fcla.edu/jon/article/view/88235>
- Nguyen TAD et al. (2017) Two known species of *Aporcelinus* Andrásy, 2009 (Dorylaimida: Aporcelaimidae) from Vietnam, with the first molecular study of the genus. *Nematology* **19**, 853–868. <http://dx.doi.org/10.1163/15685411-00003092>
- Nicholas KB, Nicholas Jr HB and Deerfield II DW (1997) GeneDoc: analysis and visualization of genetic variation. *EMBnet News* **4**, 1–14.
- Peña-Santiago R and Abolafia J (2016) On the identity of *Aporcelinus granuliferus* (Cobb, 1893) Andrásy, 2009 and its taxonomic consequences. *Nematology* **18**, 999–1014. <http://dx.doi.org/10.1163/15685411-00003011>
- Peña-Santiago R, Abolafia J and Álvarez-Ortega S (2014) New proposal for a detailed description of the dorylaimid spicule (Nematoda: Dorylaimida). *Nematology* **16**, 1091–1095. <http://dx.doi.org/10.1163/15685411-00002834>
- Ronquist F et al. (2012) MrBayes 3.2: efficient Bayesian phylogenetic inference and model choice across a large model space. *Systematic Biology* **61**, 539–542.
- Siddiqi MR (1964) Studies on *Discolaimus* spp. (Nematoda: Dorylaimidae) from India. *Zeitschrift für Zoologische Systematik und Evolutionsforschung* **2**, 174–184. <http://dx.doi.org/10.1111/j.1439-0469.1964.tb00720.x>
- Stamatakis A (2014) RAxML version 8: a tool for phylogenetic analysis and post-analysis of large phylogenies. *Bioinformatics* **30**, 1312–1313. <https://doi.org/10.1093/bioinformatics/bt0033>
- Subbotin SA et al. (2006) Phylogenetic analysis of Tylenchida Thorne, 1949 as inferred from D2 and D3 expansion fragments of the 28S rRNA gene sequences. *Nematology* **8**, 455–474. <http://dx.doi.org/10.1163/156854106778493420>
- Thompson JD et al. (1997) The ClustalX windows interface: flexible strategies for multiple sequence alignment aided by quality analysis tools. *Nucleic Acids Research* **25**, 4876–4882. <http://dx.doi.org/10.1093/nar/25.24.4876>
- Thorne G (1939) A monograph of the nematodes of the superfamily Dorylaimoidea. *Capita Zoologica* **8**, 1–261.
- Thorne G and Swanger HH (1936) A monograph of the nematode genera *Dorylaimus* Dujardin, *Aporcelaimus* n. g., *Dorylaimoides* n. g. and *Pungentus* n. g. *Capita Zoologica* **6**, 1–223.
- Varela-Benavides I and Peña-Santiago R (2018) A new species of the genus *Aporcelinus* Andrásy, 2009 (Nematoda, Dorylaimida, Aporcelaimidae) from Costa Rica. *Zootaxa* **4450**, 489–494. <http://dx.doi.org/10.11646/zootaxa.4450.4.7>
- Vinciguerra MT, Orselli L and Clausi M (2014) One new and two known species of *Aporcelinus* Andrásy, 2009 and a new species of *Coomansinema* Ahmad & Jairajpuri, 1989 (Nematoda: Dorylaimida). *Nematology* **16**, 303–322.
- Zhao CD and Zhao HH (2010) A new species of the genus *Aporcelaimellus* Heyns, 1965 – *Aporcelaimellus jiaoanensis* sp. nov. (Nematoda, Dorylaimida, Aporcelaimidae). *Acta Zootaxonomica Sinica* **35**, 876–879. (In Chinese)